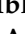*Article*

Comprehensive Analysis of Compression Ratio, Exhaust Gas Recirculation, and Pilot Fuel Injection in a Diesel Engine Fuelled with Tamarind Biodiesel

Vallapudi Dhana Raju [1], Ibham Veza [2], Harish Venu [3], Manzoore Elahi M. Soudagar [3,4,*], M. A. Kalam [5], Tansir Ahamad [6], Prabhu Appavu [7], Jayashri N. Nair [8] and S. M. Ashrafur Rahman [9,*]

[1] Department of Mechanical Engineering, Lakireddy Bali Reddy College of Engineering, Mylavaram 521230, Andhra Pradesh, India; dhanaraju1984@gmail.com
[2] Department of Mechanical Engineering, Universiti Teknologi, PETRONAS, Bandar Seri Iskandar 32610, Perak Darul Ridzuan, Malaysia; ibham.veza@utp.edu.my
[3] Institute of Sustainable Energy (ISE), Universiti Tenaga Nasional (UNITEN), Putrajaya Campus, Jalan IKRAM-UNITEN, Kajang 43000, Selangor, Malaysia; harish.venu@uniten.edu.my
[4] Department of Mechanical Engineering, Graphic Era (Deemed to Be University), Dehradun 248002, Uttarakhand, India
[5] School of Civil and Environmental Engineering, FEIT, University of Technology Sydney, Ultimo, NSW 2007, Australia; mdabul.kalam@uts.edu.au
[6] Department of Chemistry, College of Science, King Saud University, Riyadh 11421, Saudi Arabia; tahamed@ksu.edu.sa
[7] Operation & Efficiency Division, North Chennai Thermal Power Station, Chennai 600120, Tamil Nadu, India
[8] Department of Mechanical Engineering, VNR Vignana Jyothi Institute of Engineering and Technology, Hyderabad 500090, Telangana, India; jayashri@vnrvjiet.in
[9] Biofuel Engine Research Facility, Queensland University of Technology, Brisbane, QLD 4000, Australia
* Correspondence: me.soudagar@gmail.com (M.E.M.S.); rahman.ashrafur.um@gmail.com (S.M.A.R.)

Abstract: The global automotive industry is facing significant challenges, including dwindling fossil fuel reserves, rising crude oil prices, and increasingly strict emission regulations. To address these concerns, this study investigates the impact of the compression ratio (CR) and exhaust gas recirculation (EGR) on the performance and emissions of a common rail direct injection (CRDI) diesel engine fuelled with a 20% blend of tamarind seed methyl ester (TSME 20) biodiesel. The study employed an open-type electronic control unit to implement pilot fuel injection at a rate of 30%, 23° before the top dead centre (TDC), and at a higher pressure of 600 bar. Three CRs (16:1, 18:1, 20:1) and two types of EGR (hot and cold EGR at 10%) were evaluated. Diesel fuel at CR 18 was used as a baseline for comparison. The experimental procedure involved conducting tests with TSME 20 at CR 16, 18, and 20. Subsequently, TSME 20 at CR 20 + Hot EGR 10% and TSME 20 at CR 20 + Cold EGR 10% were examined. The results showed that TSME 20 operated at a higher CR (CR 20) exhibited improved diesel engine performance and significant reductions in harmful exhaust emissions. Additionally, cold EGR at 10% was more effective in reducing CO, CO_2, and NOx emissions from TSME 20 than hot EGR. The findings of this study provide valuable insights into optimizing diesel engine operation to achieve a balance between performance enhancement and emission reduction through tamarind seed biodiesel blends and different EGR techniques. The implementation of these strategies holds considerable potential in addressing the automotive industry's challenges, including ecological considerations and fuel price fluctuations.

Keywords: tamarind seed methyl ester; EGR; performance; combustion; emissions

1. Introduction

Non-renewable energy sources, such as fossil fuels, are rapidly depleting, necessitating a transition to renewable energy sources for the benefit of humanity [1,2]. The depletion of

fossil fuel resources, rising environmental pollution, and fluctuating fuel prices have motivated the adoption of biofuels such as biodiesel and bio-alcohol as promising renewable energy sources [3,4]. These fuels are considered clean, inexpensive, and abundant [5,6]. Biofuels are a crucial renewable energy source that has been extensively studied for use in diesel engines using a variety of feedstocks. These include palm oil [7], *Nigella Sativa* [8], sunflower [9], *jatropha curcas* [10], etc.

Saravanan Kumar et al. [11] investigated the impact of exhaust gas recirculation (EGR) on the performance, combustion, and emission characteristics of a diesel engine fuelled with jatropha and fish oil methyl esters. They found that the 20% blend of jatropha oil methyl ester (JOME) and fish oil methyl ester (FOME) yielded the best performance and reduced emissions with a 20% EGR rate. Kader et al. [12] studied biodiesel production using the pyrolysis process. They evaluated various fuel properties according to ASTM standards and suggested that pyrolysis oil has great potential to become the next biodiesel feedstock due to its abundance and better fuel properties.

El-Adawy et al. [13] experimentally investigated the effect of waste fry oil biodiesel blends (B0, B10, B20, and B50) at three different compression ratios (14, 16, and 18). They found that the blends performed better at the higher compression ratios. Kathirvel et al. [14] examined the effect of waste cooking oil blended with 5% ethanol and diesel in five different proportions as fuel in a variable compression ratio diesel engine. They varied the compression ratios from 18 to 22. Their results showed that a blend of 20% waste cooking oil, 5% ethanol, and 75% pure diesel exhibited the best performance and emissions characteristics at a compression ratio of 21, compared to other blends and compression ratios.

Prasad et al. [15] investigated the impact of injection timing and EGR on the attributes of a diesel engine at different load conditions. They conducted tests at various injection timings (ITs) from 19° to 27° crank angle before top dead centre (bTDC) in steps of 4 °CA. They found that retarding the injection timing by 4 °CA improved the brake thermal efficiency (BTE) by 4.07% compared to the standard operating conditions. They also observed significant reductions in CO, HC, and smoke emissions of 9.7%, 15.8%, and 6%, respectively. However, NOx emissions increased. To reduce NOx emissions, they applied 10% and 20% EGR. They reported that neat tamarind seed methyl ester (TSME) with 10% EGR resulted in a significant reduction in NOx emissions at full load. Rosha et al. [16] studied the effect of the compression ratio on a compression ignition (CI) engine fuelled with a 20% palm biodiesel blend. They varied the compression ratio in three levels: 16:1, 17:1, and 18:1. Their results showed that a compression ratio of 18:1 resulted in the highest BTE and lowest emissions. Nanthagopal et al. [17] investigated the impact of injection pressures on direct injection (DI) diesel engines fuelled with *calophyllum inophyllum* methyl ester (CIME). Their experimental results revealed that fuel consumption decreased and HC emissions decreased significantly at an injection pressure (IP) of 220 bar. However, NOx emissions increased with increasing injection pressure. Anbarasu and Karthikeyan [18] studied the effect of IP on the performance and emission characteristics of a diesel engine fuelled with canola emulsion oil. Their overall results showed a 28.8% improvement in BTE at an IP of 240 bar and a reduction in NOx emissions at an IP of 200 bar.

Mohiuddin et al. [19] investigated the impact of the compression ratio (CR) and exhaust gas recirculation (EGR) on the exhaust emissions and particulate number characteristics of diesel engines. They observed that operating a diesel engine at CR 16:1 at peak load resulted in increased thermal efficiency and decreased engine exhaust pollutants. However, they also found that increasing the CR increased NOx emissions due to the higher cylinder temperature. Shi et al. [20] examined the combined effect of CR and EGR on the various characteristics of biodiesel-fuelled diesel engines. They discovered that using 10% EGR reduces NOx and soot emissions at part load. Rajesh et al. [21] studied the influence of EGR on a compression ignition (CI) engine running on a 20% blend of jatropha biodiesel. They found that CO emissions increased by 20% and 30%, CO_2 emissions increased by 12.9% and 35%, and HC emissions increased by 14.2% and 21.4%, respectively, with 10% and 20% EGR at maximum load conditions. However, NOx emissions decreased by 20.8% and

36.9%, respectively. Table 1 summarizes the effects of hot and cold EGR on the different characteristics of CI engines.

Table 1. Influence of EGR on the diesel engine attributes.

Parameter	Fuel Blend	Operating Conditions	Inferences	References
Cold EGR of 10%, 20%, and 30%	30% blend of waste plastic biodiesel	Ideal operating conditions	The application of EGR drastically reduced the NOx emissions. However, it enhances other emissions.	Damodharan et al. [22]
15% cooled EGR	20% Karanja biodiesel	CRDI diesel engine runs at normal conditions	Particulate matter reduces and slight increase in HC emissions	Patil and Thirumalini [23]
15% hot EGR	Yellow Oleander biodiesel	Ideal operating conditions	NOx emissions were significantly reduced	Deka et al. [24]
20% and 40% hot EGR	n-pentanol-2 ethylhexyl nitrate–diesel blends	Normal operating conditions of diesel engine	NOx and soot emissions are drastically reduced. However, a slight decrement in BTE	Pan et al. [25]

Kumar et al. [26] tested diesel engines at different compression ratios (CRs) and exhaust gas recirculation (EGR) rates and found that higher CRs improved brake thermal efficiency (BTE), while 12% EGR at full load significantly reduced NOx emissions. Esakki et al. [27] produced biodiesel from leather waste and tested it with EGR rates of 5%, 10%, and 15% at full load. They found that EGR reduced CO, HC, and smoke emissions. Kumar et al. [28] observed that adding n-octanol to diesel fuel increased the ignition delay period, which improved the combustion characteristics.

De Poures et al. [29] studied the effects of a ternary blend of diesel, biodiesel, and 1-hexanol in a direct injection diesel engine. They used response surface methodology to optimize operating parameters such as fuel injection timing and EGR rate. They also found that operating the engine with 50% diesel, 30% biodiesel, and 20% 1-hexanol reduced fuel injection timing, and 10% EGR under optimal conditions improved engine performance. Jayanth et al. [30] investigated the effects of multiple injection timing and EGR on diesel engine characteristics. They found that operating a CRDI diesel engine with 10% EGR and a start of the pilot injection timing of 55° bTDC increased BTE by 1.7%, reduced NOx by 3.7%, and reduced smoke emissions by 28.9%. Sajjad et al. [31] tested different blends of soapberry biodiesel (10%, 20%, and 30%) and found that the 30% biodiesel blend had the highest BTE (27.82%), NOx emissions (1348 ppm), and HC emissions (11 ppm) at full load. Sajjad et al. [32] also tested CRDI engines with soapberry seed oil methyl ester and found that using 30% biodiesel and 30% EGR at full load improved engine parameters and reduced emissions. Kulandaivel et al. [33] studied the effects of retarded injection timing and EGR on diesel engine characteristics. They found that retarding the injection timing from 23° bTDC to 13° bTDC reduced BTE by 4.2% at full load. Additionally, using 20% EGR reduced BTE by 3.2% at full load.

The compression ratio is a key factor affecting diesel engine efficiency, power, and emissions. Biodiesel's higher cetane number allows higher compression ratios, which improves combustion efficiency and compensates for its lower energy content. This leads to more complete combustion, reducing emissions and boosting thermal efficiency. Exhaust gas recirculation (EGR) reduces NOx emissions by reintroducing exhaust gases into the intake manifold. Hot EGR lowers peak combustion temperature, reducing NOx, while cold EGR lowers particulate emissions. Biodiesel's oxygen content affects EGR, impacting NOx and smoke emissions. Optimizing the EGR rate for biodiesel blends is essential for reducing emissions without sacrificing efficiency. In diesel engines with biodiesel blends, both the compression ratio and EGR strategy significantly impact combustion efficiency, emissions, power, and fuel economy. Table 2 presents the effects of various operating parameters on diesel engine characteristics.

Table 2. Effect of engine operating parameters on diesel engine attributes.

Type of Engine	Fuel Used	Engine Operating Parameter	Inferences	References
Direct Injection diesel engine	Diesel-biodiesel-1-hexanol	Fuel Injection Timing and EGR	Improved BTE with advanced fuel injection timing and significant reduction of NOx emissions with EGR	De Poures et al. [29]
CRDI diesel engine	Waste high-density polyethylene oil	Multiple injection timing and EGR	Improved HRR and CP NOx and smoke emissions were reduced; a slight increment in BTE	Jayanth et al. [30]
CRDI diesel engine	Soapberry seed oil methyl ester	EGR variation from 10% to 30%	Drastic reduction of NOx emissions	Sajjad et al. [31]
Single cylinder water cooled diesel engine	20% Palmyra biodiesel	Compression ratio 20 and EGR 10%	Higher BTE, lower CO, HC smoke and NOx emissions	Rao and Prasad [34]
CRDI diesel engine	20% biodiesel blend	Number of nozzles and EGR	Effectively reduced HC and NOx emissions	Kim et al. [35]
CRDI diesel engine	Waste cooking biodiesel	Pilot fuel injection and EGR	Higher HC and CO emissions. However, NOx emissions were reduced	Jaliliantabar et al. [36]

Stel et al. [37] investigated the performance and flow dynamics of a centrifugal rotor operating with a gas–liquid mixture. They used the Euler-Euler polydisperse model for validation and to assess various quantities. The authors analysed the three-dimensional distribution of the gas phase inside the rotor, the gas–liquid interphase forces, the gas–liquid relative velocities, and the overall turbulence levels through the rotor.

The existing literature indicates that the compression ratio and exhaust gas recirculation (EGR) have a significant impact on the characteristics of diesel engines. However, there is a notable gap in the research regarding the effects of the compression ratio when coupled with both hot and cold EGR in the context of common rail direct injection (CRDI) diesel engines fuelled by tamarind seed methyl ester (TSME20), a blend of 20% tamarind seed methyl ester biodiesel. Given its accessibility, eco-friendliness, and cost-effectiveness, TSME holds substantial promise as a biodiesel fuel. Notably, the utilization of a 30% pilot fuel injection strategy in a CRDI diesel engine, combined with hot and cold EGR, represents an innovative approach across various operational conditions. This present study aims to investigate how different compression ratios (CR16, CR18, and CR20) and EGR methods (hot EGR at 10% and cold EGR at 10%) influence the combustion dynamics, overall engine performance, and emissions characteristics of a CRDI diesel engine running on a blend of 20% tamarind seed methyl ester biodiesel. To summarize, the current research addresses the gaps in the literature and aims to provide insights into the complex interplay between compression ratio, EGR, and the use of tamarind seed methyl ester biodiesel in a CRDI diesel engine. The findings have potential implications for improving the efficiency and environmental impact of diesel engines.

2. Material and Methods

Tamarindus indica, also known as the tamarind tree, is a widespread and abundant species in India, particularly in the states of Andhra Pradesh and Madhya Pradesh. India produces an estimated 200,000–250,000 tons of tamarind fruit annually. Tamarind trees can thrive in a variety of soil conditions with minimal water requirements. Tamarind oil is extracted from the seeds of the tamarind tree through a mechanical squeezing process. The kinematic viscosity of the extracted oil is slightly higher than that of diesel fuel, but its other properties are similar.

Tamarind oil biodiesel has several potential advantages as a sustainable and affordable alternative to traditional fossil fuels. Tamarind trees are widely cultivated in many regions, and the extraction of oil from the seeds is an eco-friendly process. Additionally,

the cultivation of tamarind trees and the extraction of oil from the seeds can be relatively cost-effective, contributing to the economic viability of tamarind oil biodiesel.

Overall, the research suggests that tamarind oil biodiesel has the potential to be a valuable alternative or supplement to conventional diesel fuel, especially in regions where tamarind trees are abundant. However, further research and development are needed to address any challenges related to the stability, storage, and long-term engine performance of tamarind oil biodiesel.

Transesterification Process

The transesterification process is the most effective method for reducing the high viscosity of biodiesel. It is also known as alcoholysis [7,38]. Transesterification is a chemical reaction that involves the removal of fatty acids and glycerol from extracted vegetable oil using a catalyst. In the transesterification process, heavy triglyceride molecules in tamarind seed oil are split into lighter and smaller straight-chain molecules. Transesterification is a well-known method for reducing the viscosity of biodiesel. It is largely affected by the free fatty acids present in the oil, the type of catalyst used, the molar ratio of reactants, and the reaction temperature. Three consecutive chemical reactions occur during the conversion of crude tamarind oil into tamarind biodiesel and glycerol. First, triglycerides are converted into diglycerides. Then, diglycerides are converted into monoglycerides. Finally, monoglycerides are converted into glycerol. The transesterification reaction process is depicted in Figure 1.
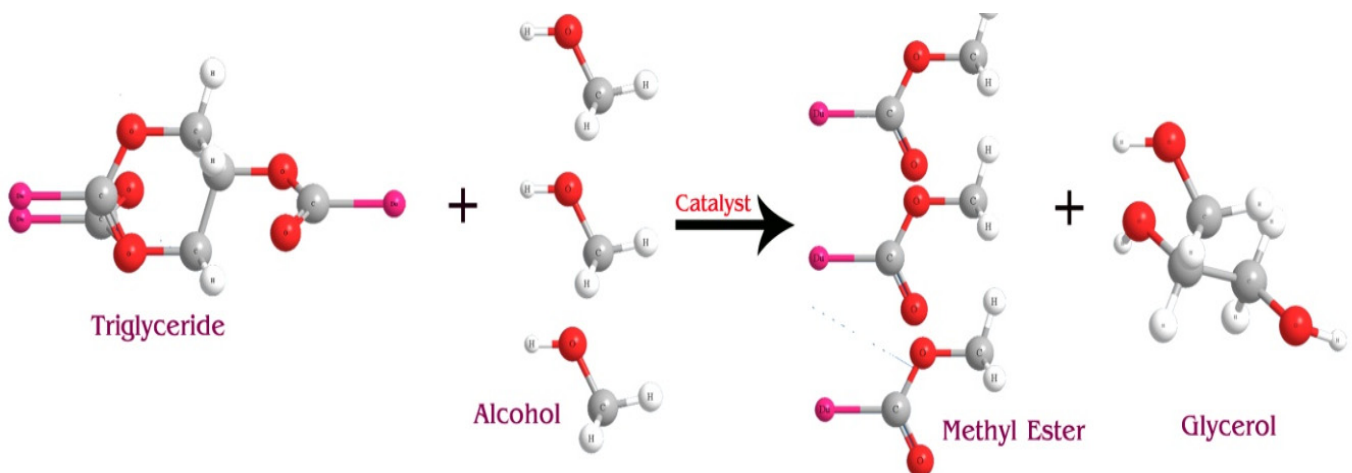

Figure 1. Transesterification chemical reaction process.

In the transesterification process, crude tamarind seed oil is thoroughly mixed with methanol, which acts as a solvent. The solution of crude oil and methanol is heated to a constant temperature of 70 °C and stirred using a magnetic stirrer. Sodium hydroxide is added at regular intervals to improve the chemical reaction. The heated solution is then cooled in the open atmosphere in a separating funnel. Two layers form in the separating funnel, with the top layer being biodiesel and the bottom layer being glycerol. To remove soap and other impurities, the tamarind seed biodiesel is washed with distilled water twice. The yield of tamarind seed oil through the transesterification process is about 92%. The different factors affecting the transesterification process are presented in Table 3, and the fuel properties of the examined samples are shown in Table 4.

Figure 2 shows the production of tamarind seed biodiesel through the transesterification process. The various physicochemical properties of tamarind biodiesel were evaluated and compared to those of diesel.

Table 3. Influencing parameters of transesterification process.

Parameter	Range of Parameters
Reaction temperature	60–300 °C
Molar ratio	5:1–40:1
Pressure	1–300 bar
Catalyst content	0.5–5%
Reaction time	1–360 min

Table 4. Various fuel properties of examined samples.

Properties	Diesel	TSME	TSME20	Test Method
Viscosity (cSt)	3.06	7.26	3.91	ASTMD 445
Density(kg/m^3)	830	882	840	ASTMD 1298
Calorific value (MJ/kg)	42.5	38.76	41.76	ASTMD 4809
Flash point (°C)	53	156	71	ASTMD 93
Fire point (°C)	58	161	75	ASTMD 93
Cetane number	45	52	46	ASTMD 613
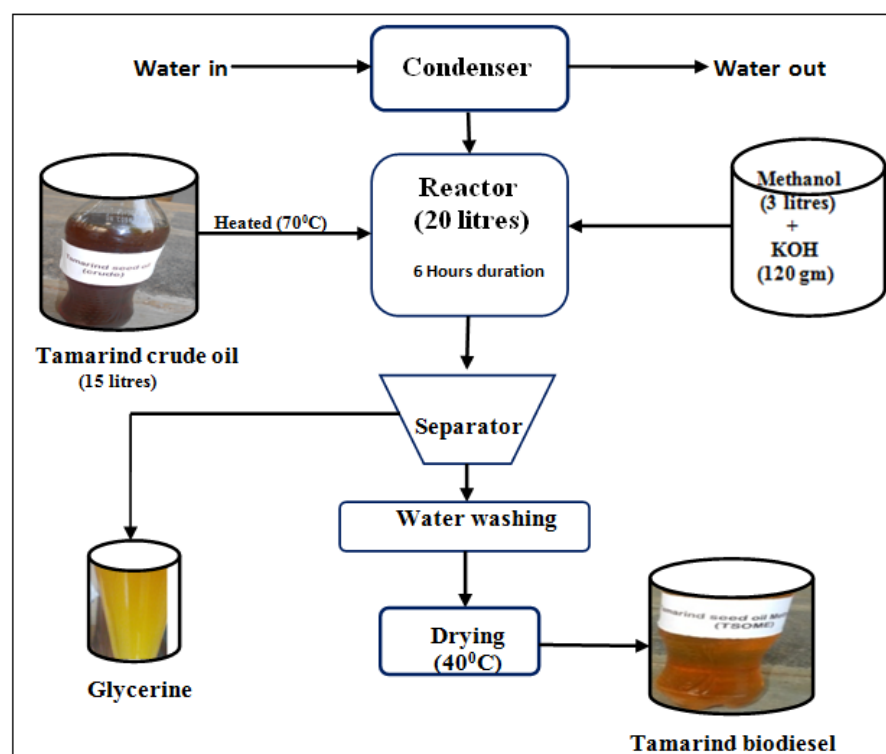
Figure 2. Transesterification process for biodiesel production.

3. Experimental Setup

This experimental investigation was conducted on a four-stroke, single-cylinder CRDI diesel engine running at a rated speed of 1500 RPM with a fuel injection timing of 23° CA bTDC. The schematic line diagram of the experimental setup is presented in Figure 3. The engine speed was maintained constant using a governing mechanism, and the load was varied using a dynamometer. The complete specifications of the tested apparatus are provided in Table 5. All necessary instruments were calibrated and used to measure various engine parameters and exhaust emissions.
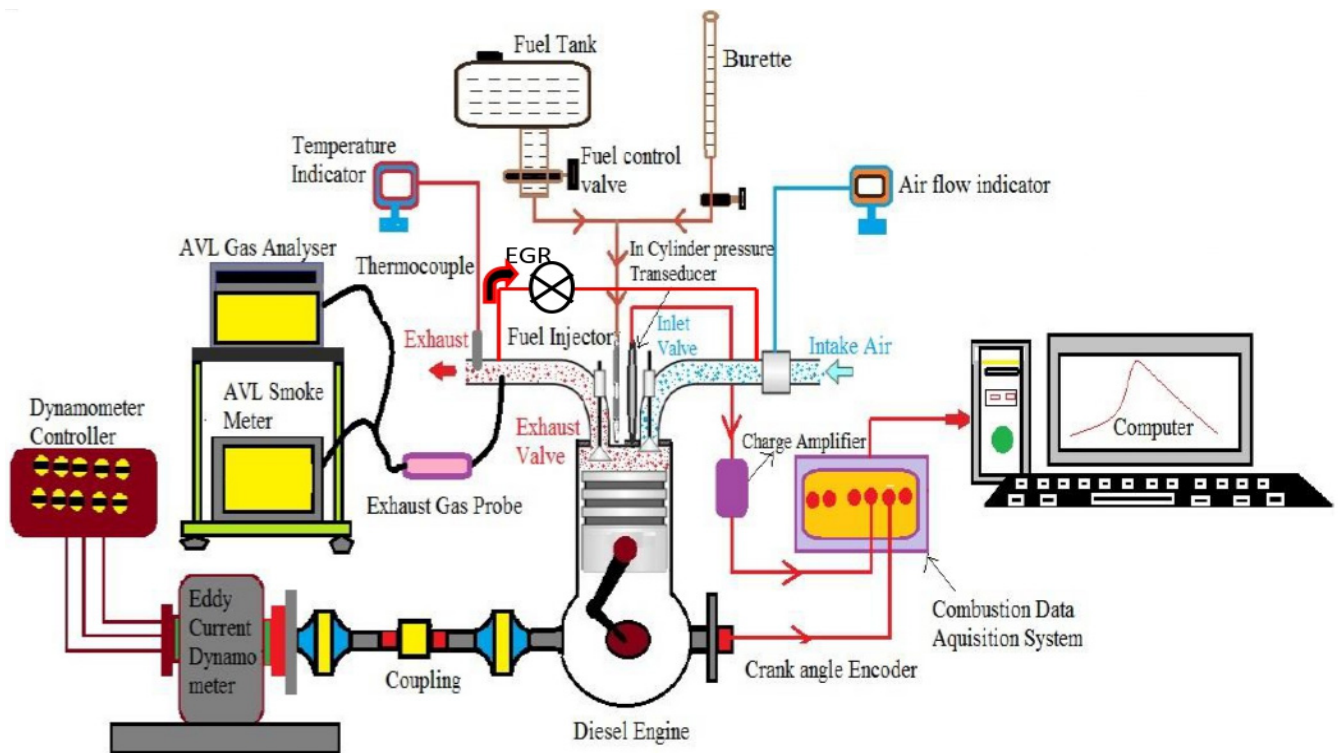
Figure 3. Schematic view of CRDI diesel engine apparatus.

Table 5. CRDI diesel engine technical specifications.

Engine Type	Kirloskar, CRDI Diesel Engine
Rated speed/power	1500 rpm/4.4 kW
Engine bore	87.5 mm
Stroke length	110 mm
No. on nozzles	03
Nozzle size	0.3 mm
Injection timing	23° CA bTDC
Combustion geometry	Hemispherical

In this study, data from the diesel engine were collected using Enginesoft4.0 combustion analysis software. This software facilitates data acquisition through four analogue and two digital inputs, which capture conditioned and multiplexed current clamp signals. The pressure transducer output, processed via a charge amplifier, TDC sensor, and crank angle encoder, was transferred to the data acquisition system (DAS) for signal conditioning. The received output signals were converted into valuable data, enabling analysis of combustion characteristics. The software also enables real-time measurement of cylinder pressure, heat release rate, fuel quantity, air flow, temperatures, and calorimeter water flow, among other variables.

The exhaust emissions from the diesel engine were measured using an AVL five-gas analyser. This analyser employs non-dispersive infrared (NDIR) spectroscopy to measure the concentrations of hydrocarbons (HC), carbon monoxide (CO), and carbon dioxide (CO_2). The smoke opacity of the engine exhaust, which is a measure of the visible part of the exhaust, was measured using an AVL smoke meter. Combustion parameters such as ignition delay period, combustion pressure (CP), and heat release rate (HRR) were measured using a LabVIEW-based IC Engine Soft 4.0 combustion analysis data acquisition system. This system uses an air-cooled piezoelectric pressure transducer (Kistler-6613 CA) to measure cylinder pressure data. The ranges, accuracies, and uncertainties of the various instruments used in the study are shown in Table 6.

Table 6. Instruments with accuracy and uncertainties.

Instrument	Parameter	Uncertainty	Accuracy
	HC	±0.2%	±2 ppm
	CO	±0.2%	±0.03%
AVL gas analyser	CO_2	±0.15%	±0.5%
	NO_X	±1%	±10 ppm
	O_2	±0.5%	±0.1%
AVL smoke meter	SO	±1%	±1%
Temperature indicator	T	±0.2%	±1 °C
Pressure transducer	P	±0.15%	±0.1 bar
Angle encoder	CA	±0.2%	±1%

Error Analysis

Error is the difference between the actual value of a quantity and its measured value. It can arise from a variety of factors, such as improper maintenance of equipment, inaccurate readings, and environmental conditions. Accurate results can only be obtained when errors are eliminated. Uncertainty is a measure of the reliability of a measurement. Error and uncertainty analysis is essential for assessing the accuracy of diesel engine characteristics.

The following mathematical Equation (1) is commonly used to calculate the combined uncertainty of multiple independent uncertainties:

$$\frac{U_y}{y} = \left[\sum_{i=1}^{n} \left(\frac{1}{y} \frac{\partial y}{\partial xi} U_{xi} \right)^2 \right]^{0.5} \tag{1}$$

where y represents a known parameter, and it is dependent on another parameter (xi)

U_y indicates the variation in y.

n is the number of parameters.

The square root method for determining the overall uncertainty of the test setup is shown in the equation below:

$$
\begin{aligned}
&= \sqrt{(\text{BSFC})^2 + (\text{BTE})^2 + (\text{HRR})^2 + (\text{CP})^2 + (\text{CO})^2 + (\text{HC})^2 + (\text{NOx})^2 + (\text{SO})^2} \\
&= \sqrt{(0.5)^2 + (0.25)^2 + (1)^2 + (1)^2 + (0.2)^2 + (0.2)^2 + (1)^2 + (1)^2} \\
&= \pm 2.09
\end{aligned}
\tag{2}
$$

4. Results and Discussion

This study investigates the effects of the compression ratio, hot exhaust gas recirculation (EGR), and cold EGR on various characteristics of a common rail direct injection (CRDI) diesel engine fuelled with a 30% pilot fuel injection of the TSME20 biodiesel blend at a fuel injection pressure of 600 bar and a rated speed of 1500 RPM. Three compression ratios (CR16, CR18, and CR20) and two types of EGR (hot and cold EGR at 10%) were investigated with TSME20. First, the engine was operated with diesel fuel at CR18 as the baseline fuel. Then, tests were conducted with TSME20 at CR16, CR18, and CR20. Finally, TSME20 at CR20 + hot EGR 10% and TSME20 at CR20 + cold EGR 10% were investigated.

4.1. Brake Specific Fuel Consumption (BSFC)

Brake specific fuel consumption (BSFC) is the amount of fuel consumed by an engine to produce one unit of brake power. The variation in BSFC with engine load for the tested fuel samples is shown in Figure 4. In general, BSFC decreases with engine load for all examined fuels. For example, at 25% engine load, the BSFC of diesel fuel is 0.45 kg/kWh, which decreases by nearly 50% to 0.24 kg/kWh at 100% engine load. The same trend is observed for other fuels, as shown in Figure 4.

Elevating the compression ratio is associated with a decrease in BSFC due to the resulting enhancement in engine efficiency. The higher compression ratio leads to a more

effective combustion process within the engine's combustion chamber. When air is compressed to a greater extent before fuel is introduced, the air–fuel mixture ignites more efficiently during the combustion stroke. This heightened efficiency results in a more complete and thorough combustion of the fuel, extracting more energy from the same amount of fuel. Consequently, less fuel is required to generate the same power output, leading to a reduction in fuel consumption as quantified by the BSFC.

This is evident in Figure 4, which shows that BSFC decreases with increasing compression ratios. For example, at 50% engine load, the BSFC of TSME20 at compression ratios of 16, 18, and 20 are 0.37, 0.34, and 0.31 kg/kWh, respectively.

In terms of EGR, cold EGR was found to have a relatively higher BSFC than hot EGR for TSME20. This is likely due to the lower temperature of cold EGR, which deteriorates the combustion process in the cylinder and increases specific fuel consumption. As reported by Damodaran et al. [22], EGR application resulted in a slight decrease in BSFC.
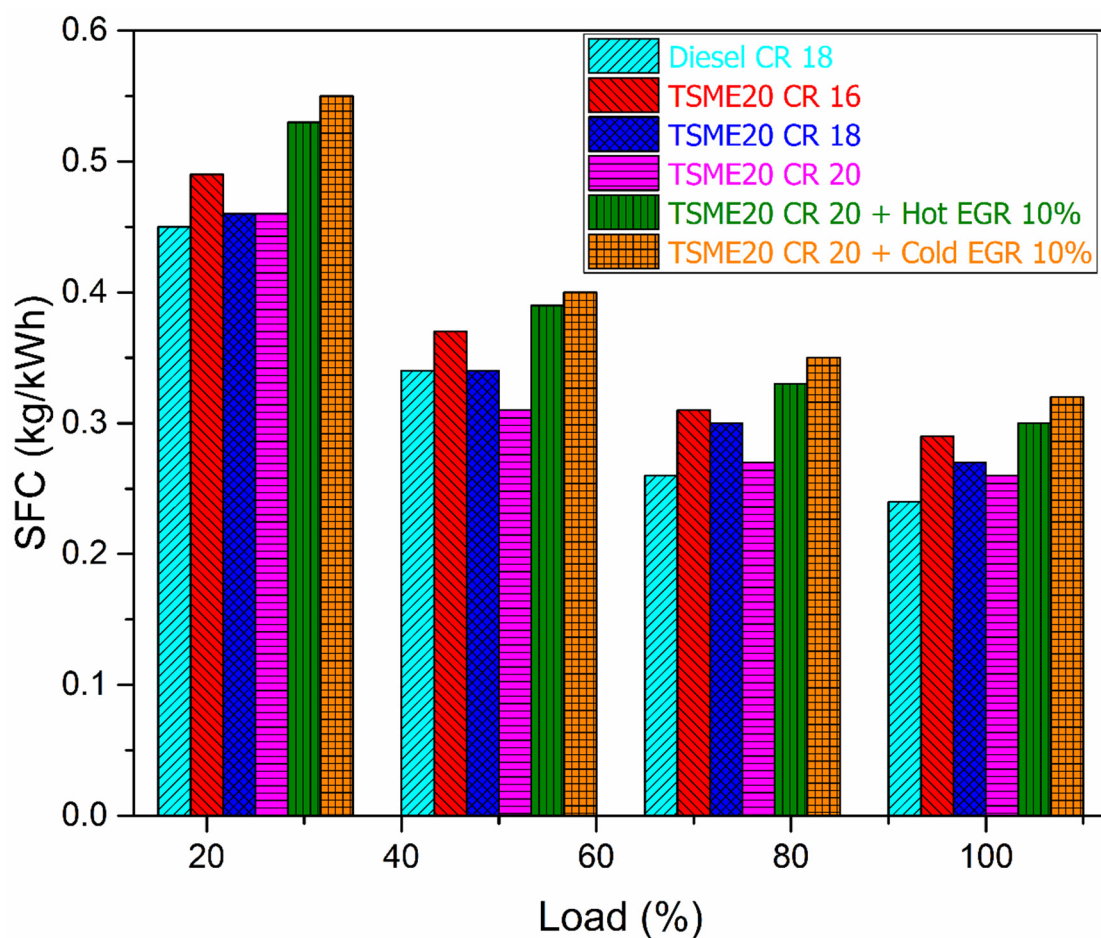

Figure 4. SFC deviation with different loads.

4.2. Brake Thermal Efficiency (BTE)

BTE is a crucial parameter of diesel engines, representing the ratio of engine power output to heat input [39]. Figure 5 depicts the variation in BTE for the examined fuels under different loads. All fuels exhibit a similar trend of increasing BTE with engine load. TSME20 CR20 recorded the highest BTE of 36.46% due to its elevated cylinder temperature at CR20, which enhanced the combustion process and improved BTE.

BTE is strongly dependent on the premixed combustion phase, and injecting 30% pilot fuel can improve fuel evaporation and fuel/air mixing, leading to better ignition at full engine load. However, the general trend of BTE increasing with the compression ratio is

not always true, as shown in Figure 5. Additionally, cold EGR 10% resulted in lower BTE than hot EGR 10% for TSME20.

Figure 5 shows that EGR has a negative effect on BTE. In each engine load, the use of EGR (both cold and hot) resulted in lower BTE compared to other blends. This could be due to the accumulation of unburned fuel and combustion by-products on the EGR valve, leading to exhaust leaking into the intake manifold. As a result, BTE decreases, and fuel consumption increases. This is supported by the previous figure (Figure 4), which shows that the blends operated in EGR have the highest BSFC. In addition to higher BSFC, exhaust leaking can also cause drivability problems.
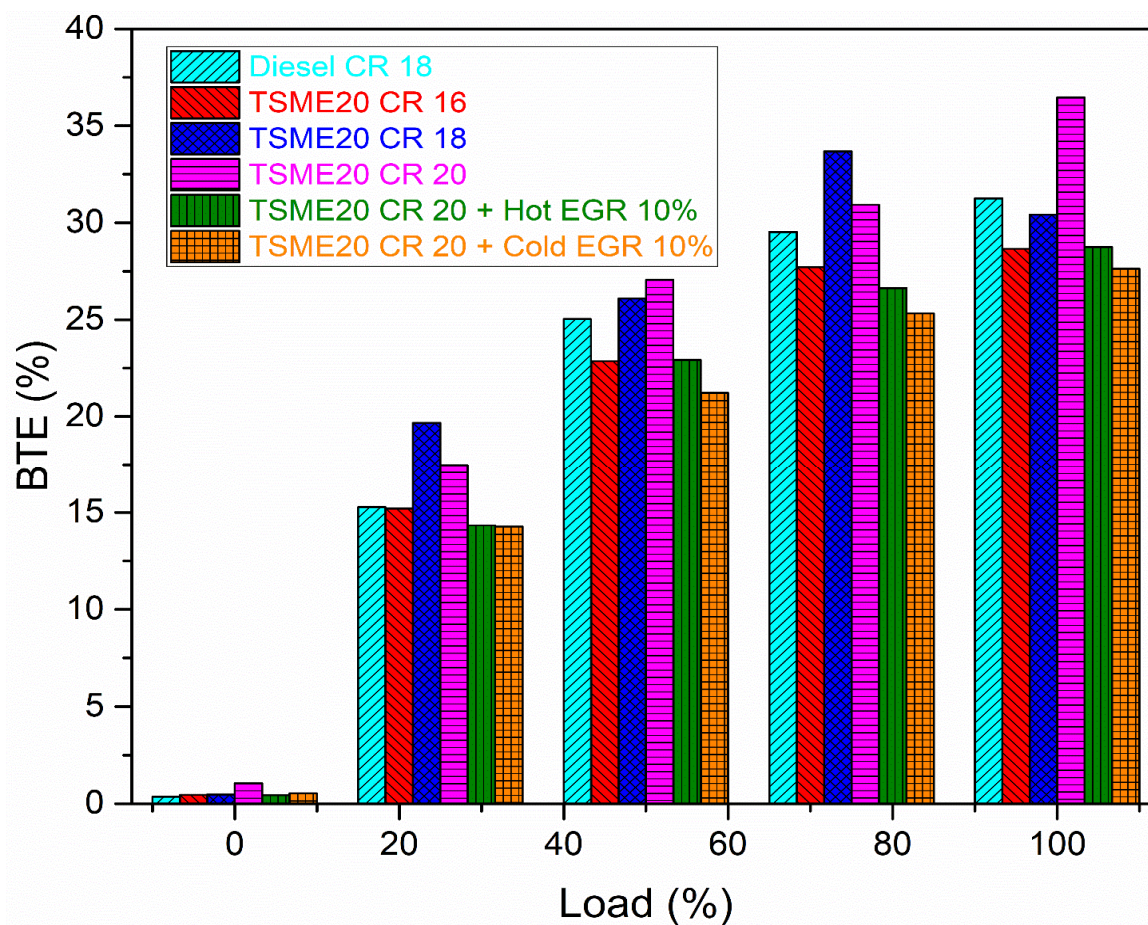

Figure 5. BTE variation with various engine loads.

4.3. In-Cylinder Pressure

In-cylinder pressure is a crucial combustion characteristic that significantly impacts engine performance and emissions [38]. The pressure development within the combustion chamber depends on the amount of fuel burned during the premixed combustion phase and the fuel–air mixing. Figure 6 shows the in-cylinder pressure variation of the investigated blends as a function of the crank angle. All curves exhibit a similar trend, with diesel fuel CR18 having the highest peak in-cylinder pressure of 74.8 bar at 5 CAD and TSME20 CR18 having the lowest value of 66.67 bar at the same crank angle.

The lower peak in-cylinder pressure of TSME blends is due to their lower calorific value than diesel fuel. Consequently, TSME blends release less combustion energy with a slower burning rate. Additionally, the slight reduction in cylinder pressure observed for TSME20 under different conditions compared to diesel is attributed to its higher viscosity, which affects fuel atomization and leads to inefficient energy use.
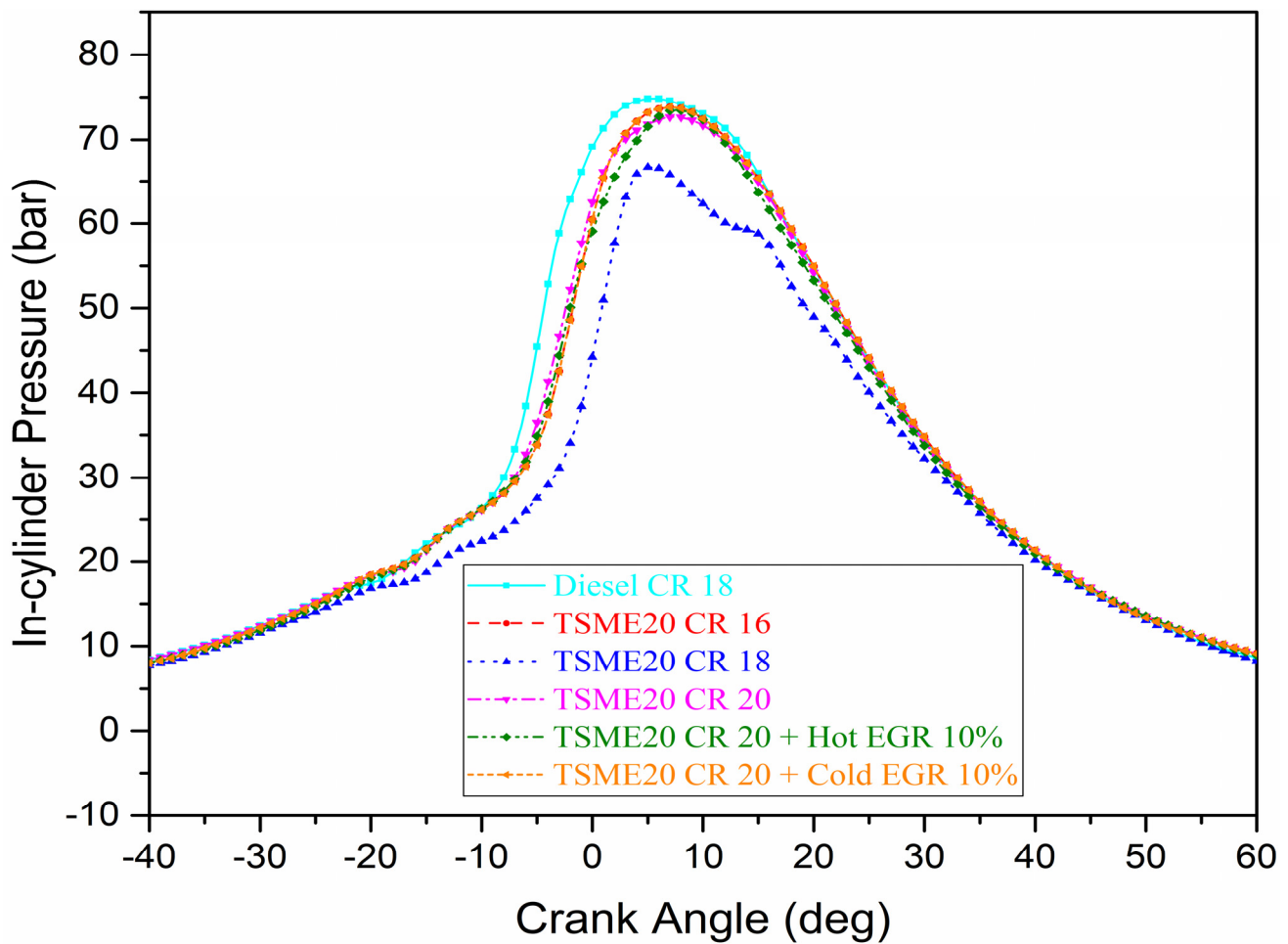
Figure 6. In-cylinder pressure variation with engine crank angle.

4.4. Heat Release Rate (HRR)

The heat release rate (HRR) is a measure of the rate at which heat is generated during combustion in an engine [40,41]. It is often used to analyse other combustion characteristics, such as ignition delay (ID) and combustion duration (CD) [42,43]. The HRR diagram is a quantitative representation of the fuel-burning process inside the cylinder and correlates with cycle efficiency and peak in-cylinder pressure. Overall, the HRR profiles of all test blends exhibit a similar trend, albeit with some fluctuations and differences in peak HRR. HRR is strongly influenced by the fuel's net energy content, as shown in Equation (3).

$$\left(\frac{dQn}{d\theta}\right) = \left(\frac{\gamma}{\gamma-1}P\frac{dV}{d\theta}\right) + \left(\frac{1}{\gamma-1}V\frac{dP}{d\theta}\right) + Q_{lw} \tag{3}$$

Figure 7 shows the variation in HRR as a function of the crank angle for the test blends. The highest peak HRR of 71.44 J/deg is observed for TSME20 CR16 at 14.32 CAD among the TSME20 biodiesel blends operated at different compression ratios. However, the diesel fuels operated at a compression ratio of 18 have a maximum HRR of 74.56 J/deg at −10 CAD at full load. This indicates that diesel fuel has a higher HRR than TSME20 biodiesel at the same compression ratio and operating conditions. It is also worth noting that the peak HRR for TSME20 CR16 occurs at a later crank angle than for diesel fuels. This is because TSME20 biodiesel has a longer ignition delay and combustion duration than diesel fuel. This is because TSME20 biodiesel has a longer ignition delay and combustion duration than diesel fuel [44,45].
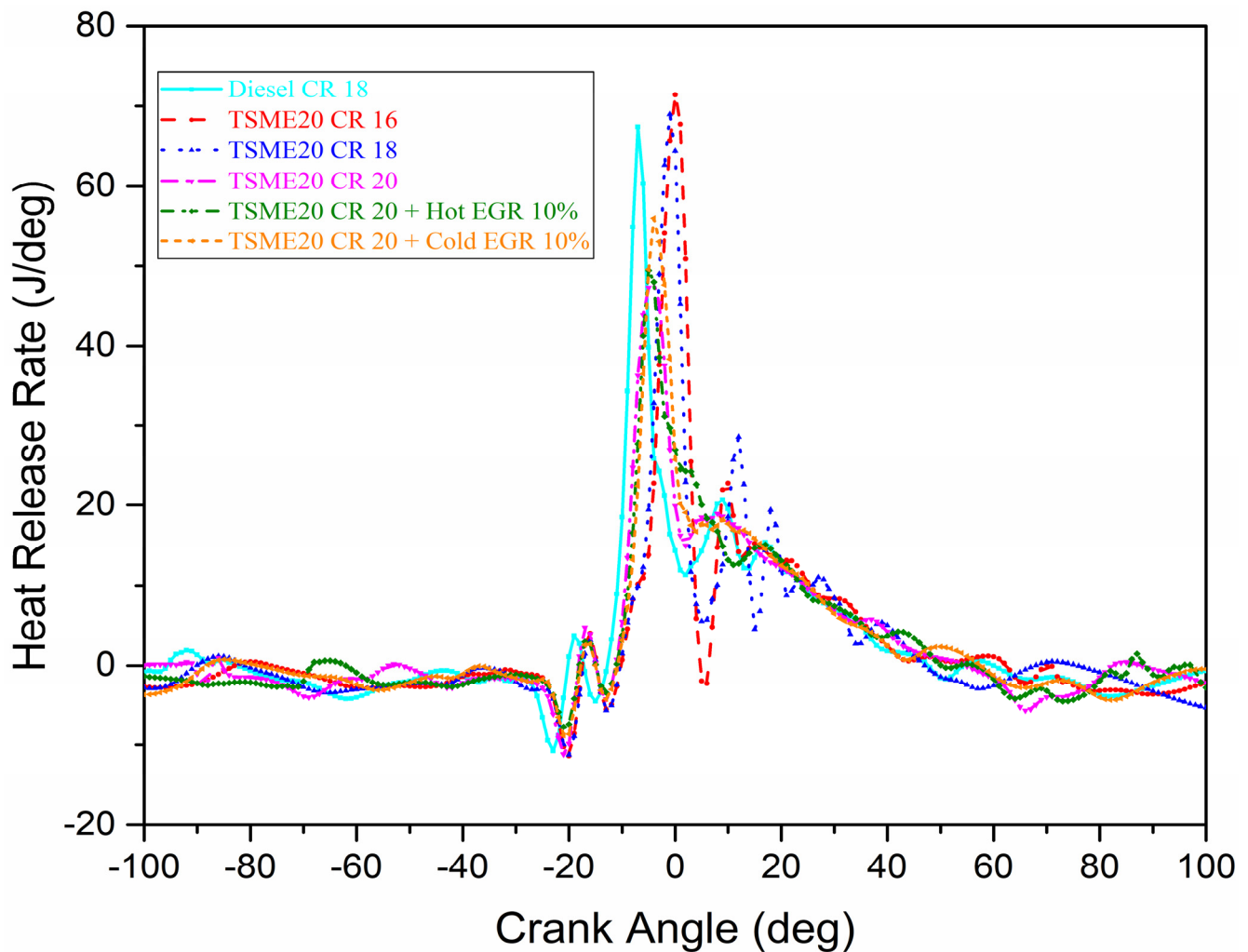
Figure 7. Variation in HRR with crank angle.

4.5. Mass Fraction of Fuel Burnt (MFB)

Mass fraction burned (MFB) is a dimensionless quantity that describes the fraction of fuel burned in a combustion engine cylinder as a function of the crank angle. It is calculated using the measured cylinder pressure and volume and provides insights into the combustion process, such as the ignition delay, combustion duration, and burn rate [46,47]. The variation in the amount of fuel burnt with the crank angle for the examined TSME20 biodiesel at different compression ratios and EGR is shown in Figure 8. It represents the rate of combustion of fuel in the engine cylinder with the crank angle period.

The MFB pattern is alike for the diesel and TSME20 at all operating conditions. Equation (4) below is used to determine the MFB.

Mass fraction of fuel burnt (MFB) =

$$MFB(\theta) = \frac{\int\limits_{\theta_{soc}}^{\theta} \left\{ \frac{\delta Q_{gen}}{d\theta} \right\} d\theta}{m_{f,total} \times \eta_{comb} \times LHV} \tag{4}$$

The rapid ignition of fuel occurs at 10–25° CA after TDC. Also, the rate of fuel burnt is increased for the TSME20 biodiesel blend with the increase in compression ratio. Also, 10% of hot exhaust gas recirculation resulted in a faster rate of combustion when compared to the 10% cold exhaust gas recirculation for the TSME20 biodiesel blend at full load.
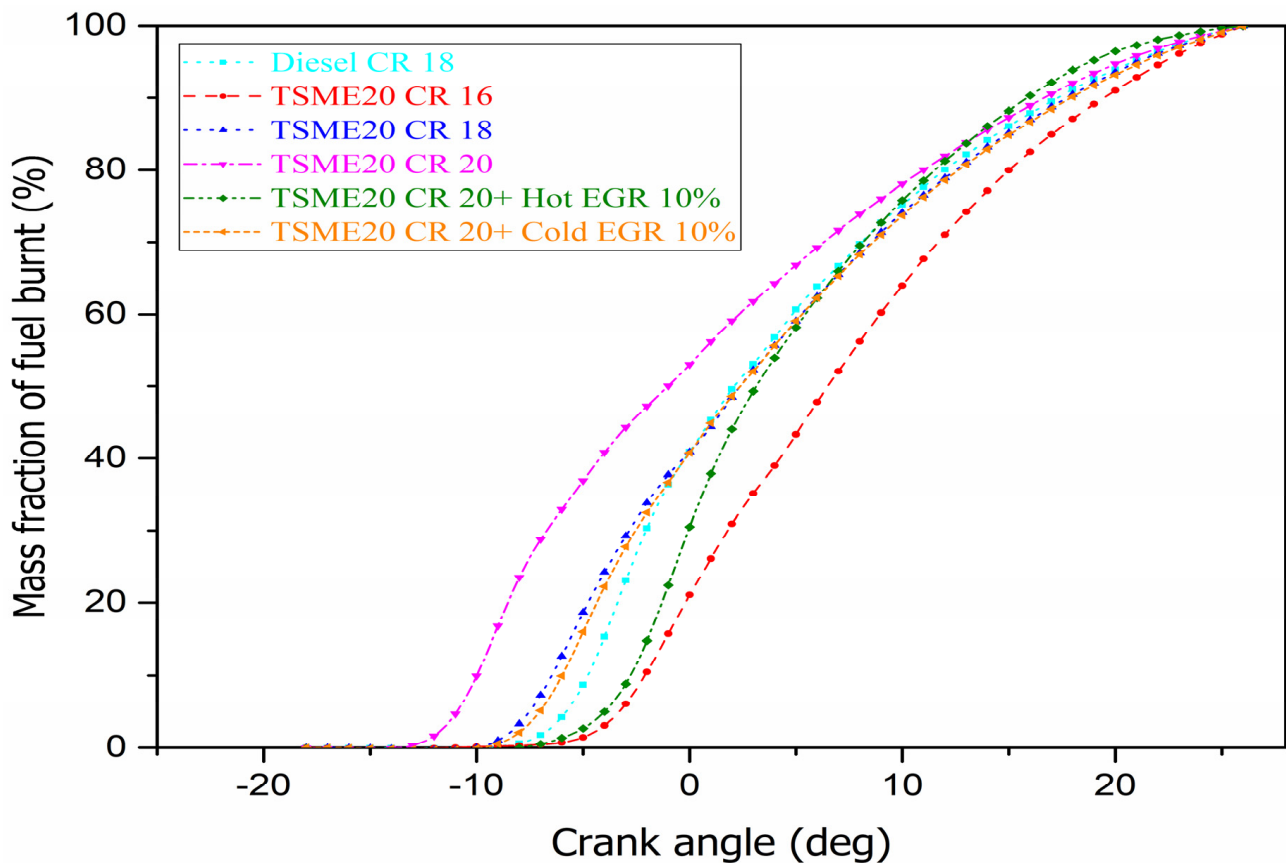
Figure 8. Variation in MFB with crank angle.

4.6. CO Emission

CO emissions are produced due to the incomplete combustion of fuel and low combustion chamber temperatures [48,49]. Poor combustion phasing caused by a lower compression ratio can also lead to higher CO emissions due to lower in-cylinder temperatures. The Cetane index and fuel viscosity are important factors that affect CO formation during the chemical reaction process [13,16]. In the absence of sufficient oxygen, CO is not fully converted to CO_2.

Figure 9 shows the variation in CO emissions with engine load for diesel fuel and TSME20 biodiesel. Interestingly, CO emissions decrease before increasing significantly close to full engine load. Except for full load, higher CO concentrations are observed at lower compression ratios. This is because the compression heat is not sufficient at low compression ratios, causing ignition delays and higher CO emissions. On the other hand, higher compression ratios result in elevated temperatures, which reduce ignition delay and facilitate more ignition processes. As a result, CO emissions are suppressed at higher compression ratios.

Furthermore, at 100% engine load, TSME20 CR20 coupled with hot EGR 10% produces the highest CO emissions, while TSME20 CR16 without EGR produces the lowest. As mentioned previously, insufficient oxygen can lead to higher CO emissions. Since EGR works by replacing fresh air with combustion products such as carbon dioxide, using EGR was found to increase CO emissions.
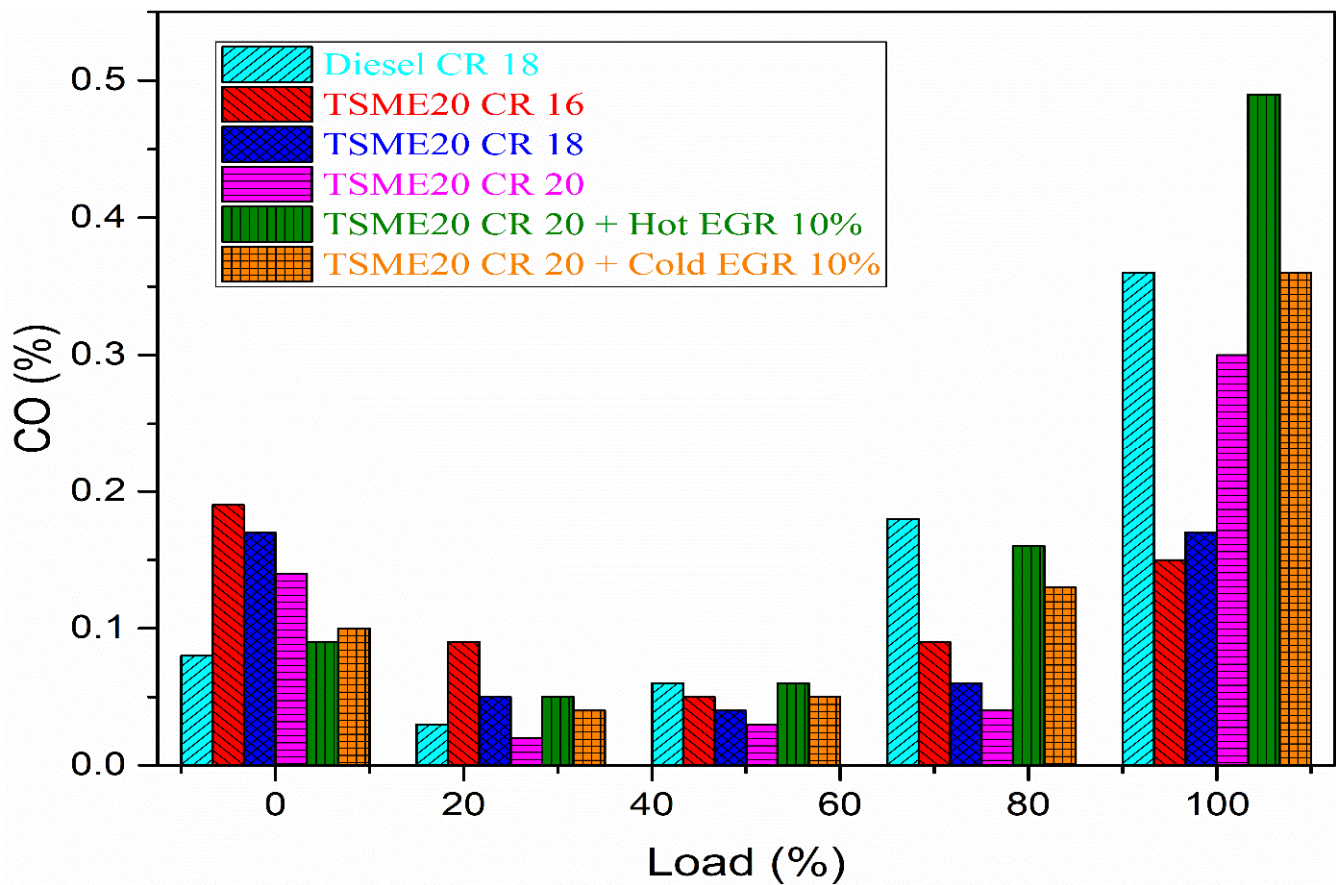
Figure 9. Variation in CO emission with different loads.

4.7. CO_2 Emission

CO$_2$ emissions were considered as indicators of completeness of the fuel's combustion inside the cylinder. When all the fuel is completely burned, CO_2 and water vapours are the only end products. The deviations in CO_2 emissions with various engine loads for the tested fuels are delineated in Figure 10. Overall, the levels of CO_2 emission increase with a similar trend as the engine load increases. The highest CO_2 emission is given by TSME20 CR20 at 7.2%, followed by TSME20 CR20 + Hot EGR 10%, TSME20 CR18, TSME20 CR20 + Cold EGR 10%, TSME20 CR 16, and Diesel CR18 at 6.9%, 6.5%, 6.1%, 5.6%, and 5.1%, respectively. It is interesting to note that CO_2 emission is consistently higher for higher compression ratios at the same load. This is due to higher heat compression at higher CRs, thus facilitating more complete combustion and converting more CO into CO_2.

As far as the EGR is concerned, Figure 10 indicates that the use of TSME20 CR20 equipped with cold EGR 10% shows relatively lower CO_2 as opposed to that of hot EGR. The EGR works by replacing the fresh air with the products of combustion, such as carbon dioxide. This results in dilution, a thermal and chemical effect that dominates the ignition timing and controls the combustion reaction rate. Cold EGR could significantly reduce more CO_2 than hot EGR because of the relatively cooler exhaust gas temperature that is re-circulated, thus having a denser concentration to decrease the oxygen content.
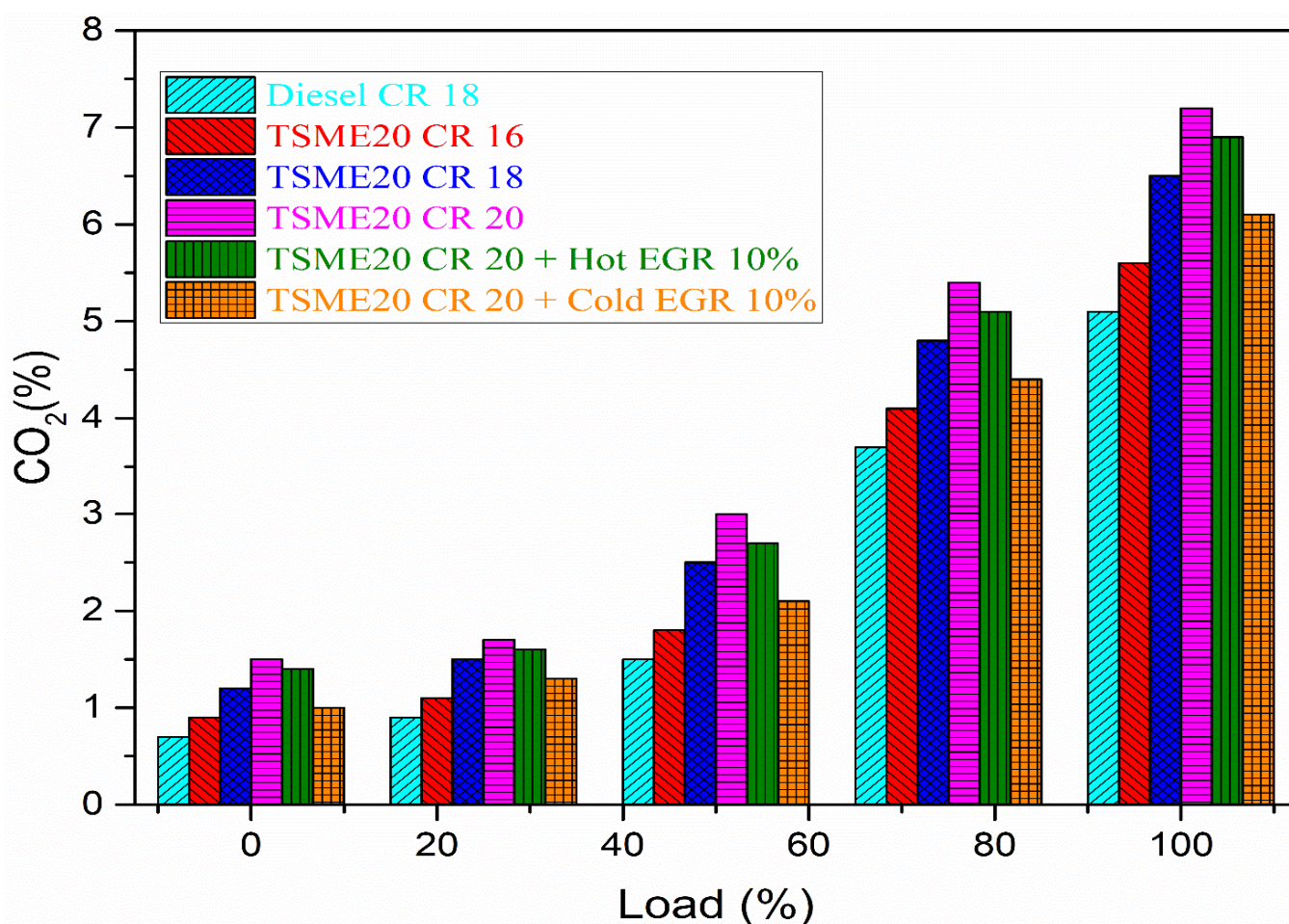
Figure 10. CO_2 variation with various loads.

4.8. HC Emission

In diesel engines, incomplete combustion and flame quenching are the primary contributors to the formation of HC emissions [50]. The relationship between HC emissions and engine load for the utilized fuels is depicted in Figure 11. Despite an initial reduction, HC emissions rise with increasing engine load, notably beyond 50% load. Under full engine load conditions, TSME20 CR20 exhibited the lowest HC emission at 31 ppm, while diesel fuel showed the highest at 69 ppm. Additionally, across all engine loads, it was noted that TSME20 CR20 with EGR at 10% exhibited comparatively lower HC emissions than when using hot EGR.

Regarding the impact of the compression ratio, the HC emission levels for TSME20 were observed to decrease with higher compression ratios. The lower in-cylinder gas temperature associated with lower compression ratios makes it challenging for the mixture to combust completely, resulting in a lean air/biodiesel mixture burning less effectively at these compression ratios. Furthermore, certain fuels may become trapped in various areas within the combustion chamber, such as the clearance between the liner and piston, thereby contributing to increased HC emissions [51].
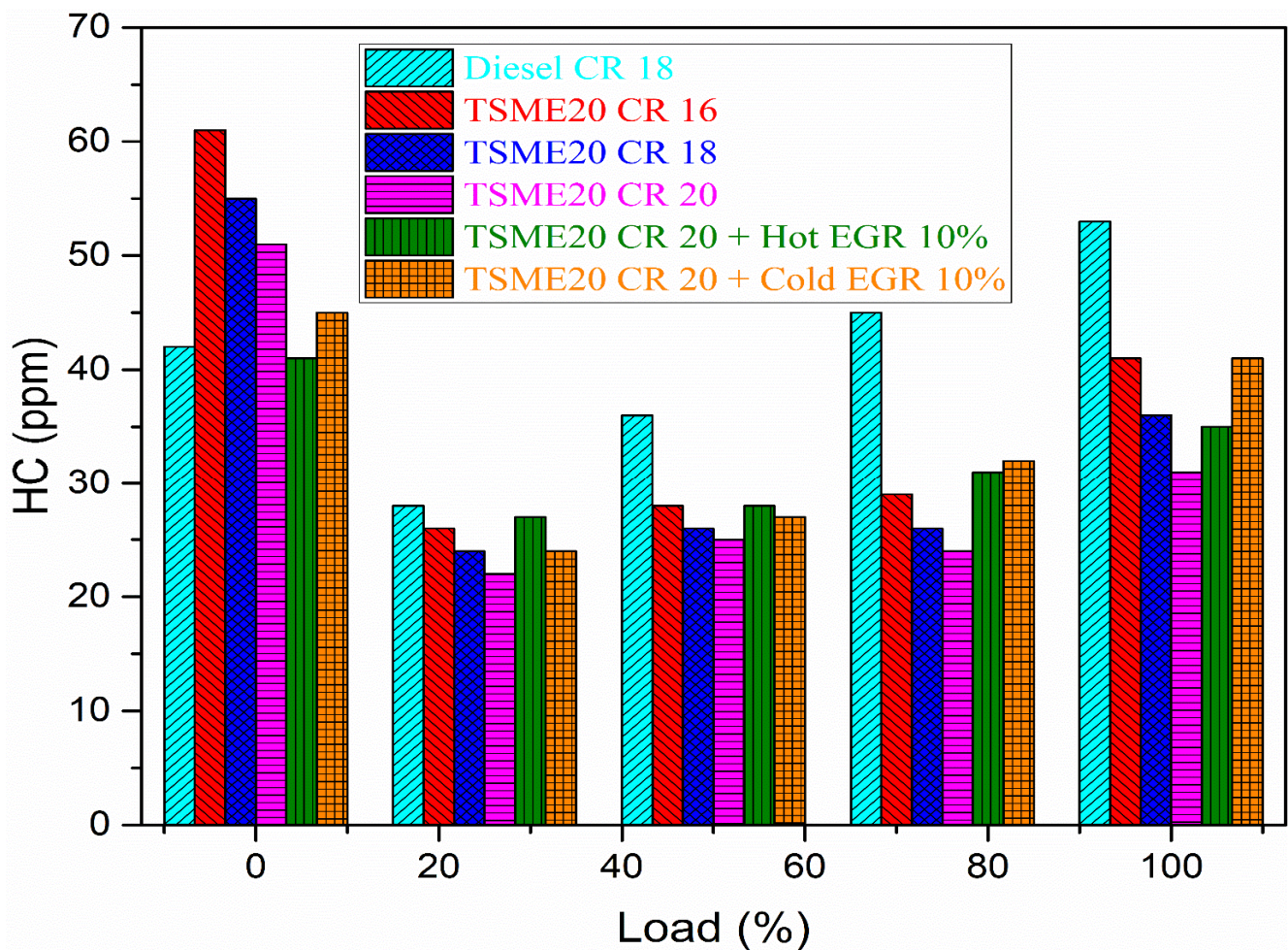
Figure 11. Variation in HC emission with different loads.

4.9. NOx Emission

NOx emission is one of the key exhaust pollutants emitted by CI engines [48,52]. NOx is typically produced at high combustion temperatures [53]. Figure 12 shows the variation in NOx emissions with engine load. NOx emissions increase linearly with engine load. This is because the fuel–air ratio (FAR) increases as the load increases, leading to higher cylinder temperatures and more generation of NOx in the engine cylinder [54]. The inherent oxygen present in TSME20 biodiesel also contributes to its higher NOx emissions. Additionally, the boiling point of tamarind biodiesel is relatively higher than that of base fuel. This means that TSME20 maintains its liquid state for a longer duration, allowing more droplets to penetrate the combustion chamber and hence resulting in higher NOx emissions. EGR can significantly reduce NOx emissions from biodiesel-fuelled diesel engines [25,27].

It is also noteworthy that NOx emissions increase significantly at higher compression ratios, while lower compression ratios produce lower NOx emissions. This is because lower in-cylinder temperatures result in reduced flame temperatures during combustion, suppressing NOx formation. The use of EGR, especially cold EGR, has also been shown to be effective in reducing NOx emissions. At full engine load, the highest level of NOx emission is liberated by TSME20 CR20 at 821 ppm, followed by TSME20 CR18, TSME20 CR16, Diesel CR18, TSME20 CR20 + Hot EGR 10%, and TSME20 CR20 + Cold EGR 10% at 762, 724, 695, 486, and 403 ppm, respectively. The use of biofuels for the diesel engine released more NOx emissions, as reported by Shi et al. [20].
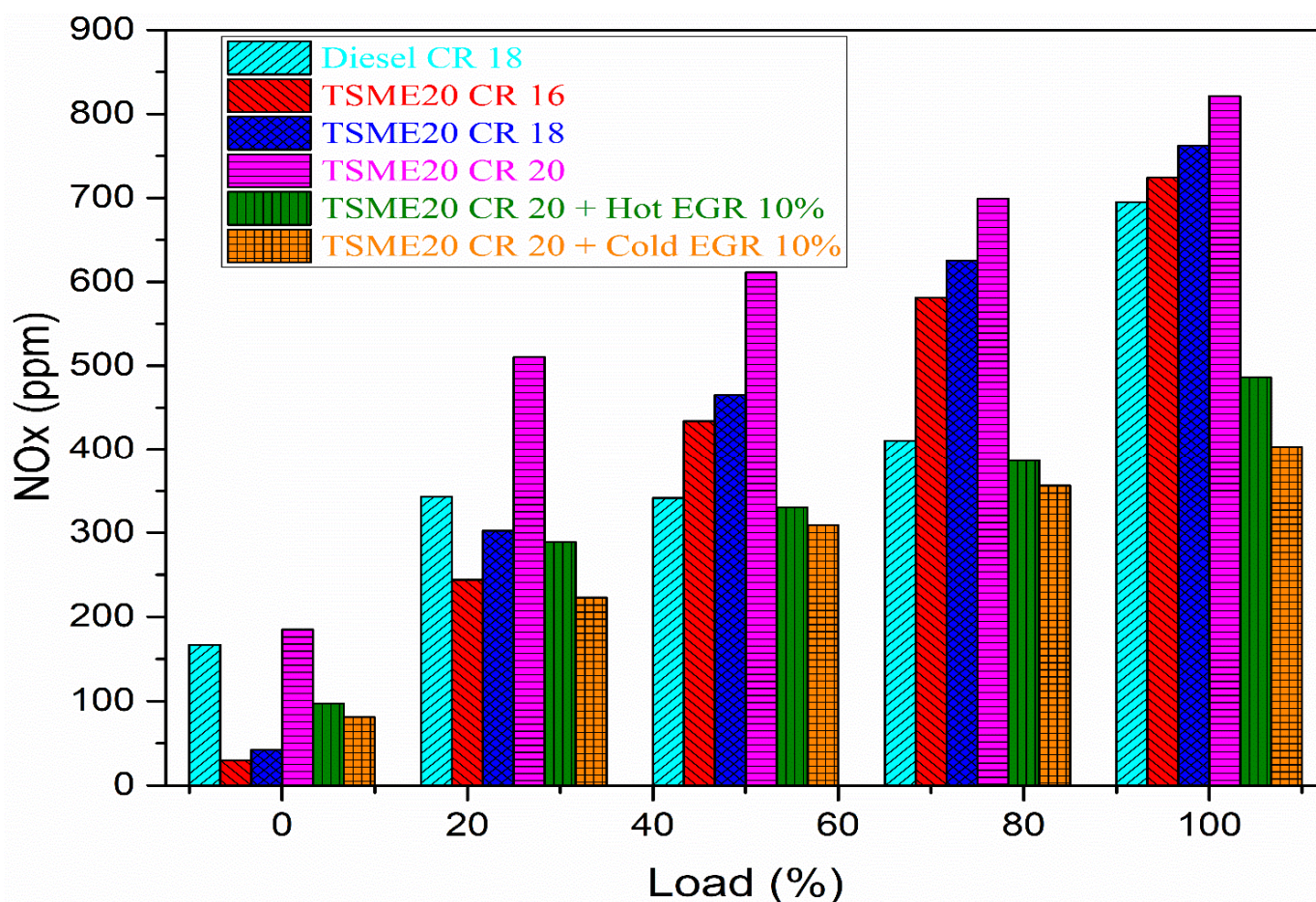
Figure 12. Nitrogen oxides emission variation with engine load.

4.10. SO Emission

Sulphur in diesel fuel has been a major problem during combustion and resulted in increased levels of the acid rain. It is important to remember that sulphur can be oxidized into SO_2 in the course of the combustion process. This can eventually form sulphurous (H_2SO_3) and sulphuric acids (H_2SO_4), which can lead to corrosive effects [37]. Yet, sulphur emissions can only be produced if there is sulphur in the blends. The variation in smoke opacity with engine load is delineated in Figure 13. Like NOx, increasing trends of SO emissions were also observed, except that their value decreases with the increasing compression ratio.

It is interesting to note that, since tamarind biodiesel has relatively lower sulphur content as opposed to diesel fuel, the SO emissions of TSME20 were reported practically lower than diesel fuel, as can be seen in Figure 13. However, the use of EGR is found to increase SO emission, especially with cold EGR. At 100% engine load, the highest SO emission is given by TSME20 CR20 + Cold EGR 10% at 69.6 ppm, followed by TSME20 CR20 + Hot EGR 10%, Diesel CR18, TSME20 CR16, TSME20 CR18, TSME20 CR20 at 66.4, 65.4, 61.6, 58.8, 57.3 ppm, respectively.
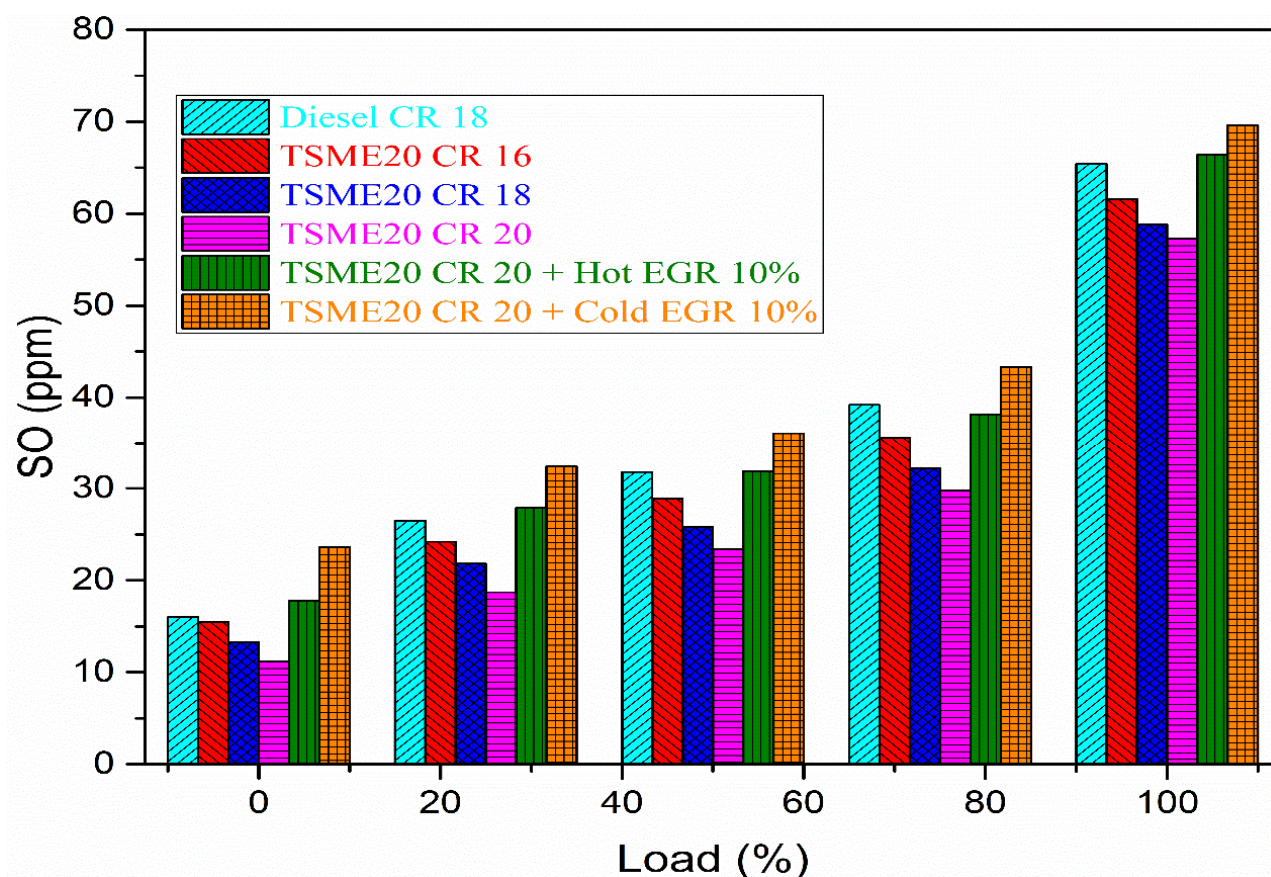
Figure 13. Variation in SO emission with different loads.

5. Conclusions

The present research delves into the impact of the compression ratio and exhaust gas recirculation (EGR) on various characteristics of a common rail direct injection (CRDI) diesel engine. This engine is powered by a blend consisting of 30% pilot fuel injection and 20% tamarind biodiesel. The key findings of this study can be summarized as follows:

➢ Tamarind biodiesel exhibits great potential as a viable source of biodiesel. Abundantly available at minimal cost, it holds the promise of being readily scalable for large-scale production.

➢ Among the different compression ratios tested for the TSME20 blend, the CR20 configuration demonstrates the highest brake thermal efficiency (BTE) at 36.46%. Comparative analysis reveals a marginal decrease in BTE due to the implementation of EGR.

➢ At higher compression ratios, the CRDI engine operating with TSME20 shows a significant decrease in fuel consumption, HC, and CO emissions. However, CO_2 and NOx emissions were found to increase due to higher in-cylinder temperature at a higher compression ratio.

➢ The introduction of cold EGR at a 10% rate proves effective in mitigating in-cylinder combustion temperatures to a sufficient degree. In comparison to the utilization of hot EGR, employing cold EGR at 10% in conjunction with the TSME20 blend demonstrates the capacity to significantly lower emissions of CO, CO_2, and NOx. However, these approaches have to compromise on elevated emissions of HC and SO.

➢ At the peak load condition, the combustion traits exhibited by the TSME20 blend, specifically, the heat release rate (HRR) and combustion pressure (CP), closely resemble the conventional diesel fuel when the engine is operated at a compression ratio of 18.

Nomenclature

BTE	Brake Thermal Efficiency
BSFC	Brake Specific Fuel Consumption
BP	Brake Power
IT	Injection Timing
EGR	Exhaust Gas Recirculation
CR	Compression Ratio
CP	Cylinder Pressure
HRR	Heat Release Rate
CO	Carbon monoxide
HC	Hydrocarbon
SO	Smoke Opacity
NOx	Nitrogen Oxides
bTDC	Before Top Dead Centre
TSME 20	20% Tamarind Seed Methyl Ester + 80% diesel
TSME 20 CR 16	TSME 20 with compression ratio 16
TSME 20 CR 18	TSME 20 with compression ratio 18
TSME 20 CR 20	TSME 20 with compression ratio 20
TSME 20 CR 20 + Hot EGR 10%	TSME 20 with compression ratio 20 with 10% Hot exhaust gas recirculation
TSME 20 CR 20 + Cold EGR 10%	TSME 20 with compression ratio 20 with 10% Cold exhaust gas recirculation

References

1. Khounani, Z.; Abdul Razak, N.N.; Hosseinzadeh-Bandbafha, H.; Madadi, M.; Sun, F.; Fattah, I.M.R.; Karimi, K.; Gupta, V.K.; Aghbashlo, M.; Tabatabaei, M. Assessing the environmental impacts of furfural production in a poplar wood biorefinery: A study on the role of mannitol concentration and catalyst type. *Ind. Crops Prod.* **2023**, *203*, 117230. [CrossRef]
2. Ejaz, A.; Babar, H.; Ali, H.M.; Jamil, F.; Janjua, M.M.; Fattah, I.M.R.; Said, Z.; Li, C. Concentrated photovoltaics as light harvesters: Outlook, recent progress, and challenges. *Sustain. Energy Technol. Assess.* **2021**, *46*, 101199. [CrossRef]
3. Santhosh, N.; Afzal, A.; Ağbulut, Ü.; Alahmadi, A.A.; Gowda, A.C.; Alwetaishi, M.; Shaik, S.; Hoang, A.T. Poultry fat biodiesel as a fuel substitute in diesel-ethanol blends for DI-CI engine: Experimental, modeling and optimization. *Energy* **2023**, *270*, 126826.
4. Sarıdemir, S.; Ağbulut, Ü. Combustion, performance, vibration and noise characteristics of cottonseed methyl ester–diesel blends fuelled engine. *Biofuels* **2019**, *13*, 201–210. [CrossRef]
5. Ong, H.C.; Tiong, Y.W.; Goh, B.H.H.; Gan, Y.Y.; Mofijur, M.; Fattah, I.M.R.; Chong, C.T.; Alam, M.A.; Lee, H.V.; Silitonga, A.S.; et al. Recent advances in biodiesel production from agricultural products and microalgae using ionic liquids: Opportunities and challenges. *Energy Convers. Manag.* **2021**, *228*, 113647. [CrossRef]
6. Hoang, A.T.; Ong, H.C.; Fattah, I.M.R.; Chong, C.T.; Cheng, C.K.; Sakthivel, R.; Ok, Y.S. Progress on the lignocellulosic biomass pyrolysis for biofuel production toward environmental sustainability. *Fuel Process. Technol.* **2021**, *223*, 106997. [CrossRef]
7. Fattah, I.M.R.; Ong, H.C.; Mahlia, T.M.I.; Mofijur, M.; Silitonga, A.S.; Rahman, S.M.A.; Ahmad, A. State of the Art of Catalysts for Biodiesel Production. *Front. Energy Res.* **2020**, *8*, 101. [CrossRef]
8. Yunus Khan, T.M.; Atabani, A.E.; Badruddin, I.A.; Ankalgi, R.F.; Mainuddin Khan, T.K.; Badarudin, A. Ceiba pentandra, Nigella sativa and their blend as prospective feedstocks for biodiesel. *Ind. Crops Prod.* **2015**, *65*, 367–373. [CrossRef]
9. Elkelawy, M.; Bastawissi, H.A.-E.; Esmaeil, K.K.; Radwan, A.M.; Panchal, H.; Sadasivuni, K.K.; Suresh, M.; Israr, M. Maximization of biodiesel production from sunflower and soybean oils and prediction of diesel engine performance and emission characteristics through response surface methodology. *Fuel* **2020**, *266*, 117072. [CrossRef]

10. Dharma, S.; Hassan, M.H.; Ong, H.C.; Sebayang, A.H.; Silitonga, A.S.; Kusumo, F.; Milano, J. Experimental study and prediction of the performance and exhaust emissions of mixed Jatropha curcas-Ceiba pentandra biodiesel blends in diesel engine using artificial neural networks. *J. Clean. Prod.* **2017**, *164*, 618–633. [CrossRef]

11. Kumar, M.S.; Prabhahar, M.; Sendilvelan, S.; Singh, S.; Venkatesh, R.; Bhaskar, K. Combustion, performance and emission analysis of a diesel engine fueled with methyl esters of Jatropha and fish oil with exhaust gas recirculation. *Energy Procedia* **2019**, *160*, 404–411. [CrossRef]

12. Kader, M.; Islam, M.; Parveen, M.; Haniu, H.; Takai, K. Pyrolysis decomposition of tamarind seed for alternative fuel. *Bioresour. Technol.* **2013**, *149*, 1–7. [CrossRef] [PubMed]

13. El-Adawy, M.; El-Kasaby, M.; Eldrainy, Y.A. Performance characteristics of a supercharged variable compression ratio diesel engine fueled by biodiesel blends. *Alex. Eng. J.* **2018**, *57*, 3473–3482. [CrossRef]

14. Kathirvel, S.; Layek, A.; Muthuraman, S. Performance characteristics of CI engine using blends of waste cooking oil methyl ester, ethanol and diesel. *Int. J. Ambient. Energy* **2020**, *41*, 570–581. [CrossRef]

15. Bala Prasad, K.; Dhana Raju, V.; Ahamad Shaik, A.; Gopidesi, R.K.; Sreekara Reddy, M.B.S.; Soudagar, M.E.M.; Mujtaba, M.A. Impact of injection timings and exhaust gas recirculation rates on the characteristics of diesel engine operated with neat tamarind biodiesel. *Energy Sources Part A Recovery Util. Environ. Eff.* **2021**, 1–19. [CrossRef]

16. Rosha, P.; Mohapatra, S.K.; Mahla, S.K.; Cho, H.; Chauhan, B.S.; Dhir, A. Effect of compression ratio on combustion, performance, and emission characteristics of compression ignition engine fueled with palm (B20) biodiesel blend. *Energy* **2019**, *178*, 676–684. [CrossRef]

17. Nanthagopal, K.; Ashok, B.; Raj, R.T.K. Influence of fuel injection pressures on Calophyllum inophyllum methyl ester fuelled direct injection diesel engine. *Energy Convers. Manag.* **2016**, *116*, 165–173. [CrossRef]

18. Anbarasu, A.; Karthikeyan, A. Effect of injection pressure on the performance and emission characteristics of CI engine using canola emulsion fuel. *Int. J. Ambient. Energy* **2017**, *38*, 314–319. [CrossRef]

19. Mohiuddin, K.; Kwon, H.; Choi, M.; Park, S. Effect of engine compression ratio, injection timing, and exhaust gas recirculation on gaseous and particle number emissions in a light-duty diesel engine. *Fuel* **2021**, *294*, 120547. [CrossRef]

20. Shi, X.; Liu, B.; Zhang, C.; Hu, J.; Zeng, Q. A study on combined effect of high EGR rate and biodiesel on combustion and emission performance of a diesel engine. *Appl. Therm. Eng.* **2017**, *125*, 1272–1279. [CrossRef]

21. Kumar, V.; Mahla, S.K. Influence of EGR on a CI engine running on 20% blend of jatropha biodiesel. *Mater. Today Proc.* **2021**, *43*, 273–280.

22. Damodharan, D.; Sathiyagnanam, A.P.; Rajesh Kumar, B.; Ganesh, K.C. Cleaner emissions from a DI diesel engine fueled with waste plastic oil derived from municipal solid waste under the influence of n-pentanol addition, cold EGR, and injection timing. *Environ. Sci. Pollut. Res.* **2018**, *25*, 13611–13625. [CrossRef] [PubMed]

23. Patil, V.; Thirumalini, S. Effect of cooled EGR on performance and emission characteristics of diesel engine with diesel and diesel-karanja blend. *Mater. Today Proc.* **2021**, *46*, 4720–4727. [CrossRef]

24. Deka, M.; Mahanta, P.K.; Choudhury, N.D. Effect of EGR on Performance and Emission Characteristics of a Diesel Engine Fueled with Yellow Oleander Seed Oil Biodiesel. In *Advances in Thermofluids and Renewable Energy: Select Proceedings of TFRE 2020*; Springer: Singapore, 2020; pp. 351–363.

25. Pan, M.; Huang, R.; Liao, J.; Ouyang, T.; Zheng, Z.; Lv, D.; Huang, H. Effect of EGR dilution on combustion, performance and emission characteristics of a diesel engine fueled with n-pentanol and 2-ethylhexyl nitrate additive. *Energy Convers. Manag.* **2018**, *176*, 246–255. [CrossRef]

26. Kumar, P.V.; Ashok, B.; Vignesh, R.; Bhasker, J.P.; Kumar, A.N. Evaluation of performance, emissions and combustion attributes of CI engine using palmyra biodiesel blend with distinct compression ratios, EGR rates and nano-particles. *Fuel* **2022**, *321*, 124092. [CrossRef]

27. Esakki, T.; Rangaswamy, S.M.; Jayabal, R. An experimental study on biodiesel production and impact of EGR in a CRDI diesel engine propelled with leather industry waste fat biodiesel. *Fuel* **2022**, *321*, 123995. [CrossRef]

28. Kumar, B.R.; Saravanan, S.; Rana, D.; Nagendran, A. Combined effect of injection timing and exhaust gas recirculation (EGR) on performance and emissions of a DI diesel engine fuelled with next-generation advanced biofuel–diesel blends using response surface methodology. *Energy Convers. Manag.* **2016**, *123*, 470–486. [CrossRef]

29. De Poures, M.V.; Dillikannan, D.; Kaliyaperumal, G.; Thanikodi, S.; Ağbulut, Ü.; Hoang, A.T.; Mahmoud, Z.; Shaik, S.; Saleel, C.A.; Afzal, A. Collective influence and optimization of 1-hexanol, fuel injection timing, and EGR to control toxic emissions from a light-duty agricultural diesel engine fueled with diesel/waste cooking oil methyl ester blends. *Process Saf. Environ. Prot.* **2023**, *172*, 738–752. [CrossRef]

30. Jayanth, B.V.; Depoures, M.V.; Kaliyaperumal, G.; Dillikannan, D.; Jawahar, D.; Palani, K.; Shivappa, G.P.M. A comprehensive study on the effects of multiple injection strategies and exhaust gas recirculation on diesel engine characteristics that utilize waste high density polyethylene oil. *Energy Sources Part A Recovery Util. Environ. Eff.* **2021**, 1–18. [CrossRef]

31. Sajjad, M.O.A.; Sathish, T.; Saravanan, R.; Asif, M.; Linul, E.; Ağbulut, Ü. Combustion, performance and emission discussion of soapberry seed oil methyl ester blends and exhaust gas recirculation in common rail direct fuel injection system. *Energy* **2023**, *278*, 127763. [CrossRef]

32. Sajjad, M.O.A.; Sathish, T.; Rajasimman, M.; Praveenkumar, T. Experimental evaluation of soapberry seed oil biodiesel performance in CRDI diesel engine. *Sci. Rep.* **2023**, *13*, 5699. [CrossRef]

33. Kulandaivel, D.; Rahamathullah, I.; Sathiyagnanam, A.; Gopal, K.; Damodharan, D. Effect of retarded injection timing and EGR on performance, combustion and emission characteristics of a CRDi diesel engine fueled with WHDPE oil/diesel blends. *Fuel* **2020**, *278*, 118304. [CrossRef]

34. Rao, G.P.; Prasad, L.S.V. Combined influence of compression ratio and exhaust gas recirculation on the diverse characteristics of the diesel engine fueled with novel palmyra biodiesel blend. *Energy Convers. Manag. X* **2022**, *14*, 100185.

35. Kim, T.; Park, J.; Cho, H. Emission characteristics under diesel and biodiesel fueled compression ignition engine with various injector holes and EGR conditions. *Energies* **2020**, *13*, 2973. [CrossRef]

36. Jaliliantabar, F.; Ghobadian, B.; Carlucci, A.P.; Najafi, G.; Mamat, R.; Ficarella, A.; Strafella, L.; Santino, A.; De Domenico, S. A comprehensive study on the effect of pilot injection, EGR rate, IMEP and biodiesel characteristics on a CRDI diesel engine. *Energy* **2020**, *194*, 116860. [CrossRef]

37. Stel, H.; Ofuchi, E.M.; Chiva, S.; Morales, R.E.M. Numerical assessment of performance characteristics and two-phase flow dynamics of a centrifugal rotor operating under gas entrainment condition. *Exp. Comput. Multiph. Flow* **2022**, *4*, 221–240. [CrossRef]

38. Veza, I.; Afzal, A.; Mujtaba, M.A.; Tuan Hoang, A.; Balasubramanian, D.; Sekar, M.; Fattah, I.M.R.; Soudagar, M.E.M.; El-Seesy, A.I.; Djamari, D.W.; et al. Review of artificial neural networks for gasoline, diesel and homogeneous charge compression ignition engine. *Alex. Eng. J.* **2022**, *61*, 8363–8391. [CrossRef]

39. Atmanli, A.; Ileri, E.; Yilmaz, N. Optimization of diesel–butanol–vegetable oil blend ratios based on engine operating parameters. *Energy* **2016**, *96*, 569–580. [CrossRef]

40. Wang, Z.; Zhang, T.; Huang, X. Predicting real-time fire heat release rate by flame images and deep learning. *Proc. Combust. Inst.* **2023**, *39*, 4115–4123. [CrossRef]

41. Zhou, T.; Tang, P.; Ye, T. Machine learning based heat release rate indicator of premixed methane/air flame under wide range of equivalence ratio. *Energy* **2023**, *263*, 126103. [CrossRef]

42. Singh Pali, H.; Sharma, A.; Kumar, M.; Anand Annakodi, V.; Nhanh Nguyen, V.; Kumar Singh, N.; Singh, Y.; Balasubramanian, D.; Deepanraj, B.; Hai Truong, T.; et al. Enhancement of combustion characteristics of waste cooking oil biodiesel using TiO_2 nanofluid blends through RSM. *Fuel* **2023**, *331*, 125681. [CrossRef]

43. Ouchikh, S.; Lounici, M.S.; Tarabet, L.; Loubar, K.; Tazerout, M. Effect of natural gas enrichment with hydrogen on combustion characteristics of a dual fuel diesel engine. *Int. J. Hydrog. Energy* **2019**, *44*, 13974–13987. [CrossRef]

44. Azad, A.K.; Rasul, M.G.; Bhatt, C. Combustion and emission analysis of Jojoba biodiesel to assess its suitability as an alternative to diesel fuel. *Energy Procedia* **2019**, *156*, 159–165. [CrossRef]

45. Huang, J.; Xiao, H.; Yang, X.; Guo, F.; Hu, X. Effects of methanol blending on combustion characteristics and various emissions of a diesel engine fueled with soybean biodiesel. *Fuel* **2020**, *282*, 118734. [CrossRef]

46. Kaya, G. Experimental comparative study on combustion, performance and emissions characteristics of ethanol-gasoline blends in a two stroke uniflow gasoline engine. *Fuel* **2022**, *317*, 120917. [CrossRef]

47. Kavitha, M.S.; Murugavelh, S. Optimization and transesterification of sterculia oil: Assessment of engine performance, emission and combustion analysis. *J. Clean. Prod.* **2019**, *234*, 1192–1209. [CrossRef]

48. Hazar, H.; Telceken, T.; Sevinc, H. An experimental study on emission of a diesel engine fuelled with SME (safflower methyl ester) and diesel fuel. *Energy* **2022**, *241*, 122915. [CrossRef]

49. Cengiz, C.; Unverdi, S.O. A CFD Study on the Effects of Injection Timing and Spray Inclusion Angle on Performance and Emission Characteristics of a DI Diesel Engine Operating in Diffusion-Controlled and PCCI Modes of Combustion. *Energies* **2023**, *16*, 2861. [CrossRef]

50. Dhana Raju, V.; Nair, J.N.; Venu, H.; Subramani, L.M.; Soudagar, M.E.; Mujtaba, M.A.; Khan, T.M.Y.; Ismail, K.A.; Elfasakhany, A.; Yusuf, A.A.; et al. Combined assessment of injection timing and exhaust gas recirculation strategy on the performance, emission and combustion characteristics of algae biodiesel powered diesel engine. *Energy Sources Part A Recovery Util. Environ. Eff.* **2022**, *44*, 8554–8571. [CrossRef]

51. Doppalapudi, A.T.; Azad, A.K.; Khan, M.M.K. Combustion chamber modifications to improve diesel engine performance and reduce emissions: A review. *Renew. Sustain. Energy Rev.* **2021**, *152*, 111683. [CrossRef]

52. Mofijur, M.; Fattah, I.M.R.; Alam, M.A.; Islam, A.B.M.S.; Ong, H.C.; Rahman, S.M.A.; Najafi, G.; Ahmed, S.F.; Uddin, M.A.; Mahlia, T.M.I. Impact of COVID-19 on the social, economic, environmental and energy domains: Lessons learnt from a global pandemic. *Sustain. Prod. Consum.* **2021**, *26*, 343–359. [CrossRef] [PubMed]

53. Ming, C.; Rizwanul Fattah, I.M.; Chan, Q.N.; Pham, P.X.; Medwell, P.R.; Kook, S.; Yeoh, G.H.; Hawkes, E.R.; Masri, A.R. Combustion characterization of waste cooking oil and canola oil based biodiesels under simulated engine conditions. *Fuel* **2018**, *224*, 167–177. [CrossRef]

54. Frost, J.; Tall, A.; Sheriff, A.M.; Schönborn, A.; Hellier, P. An experimental and modelling study of dual fuel aqueous ammonia and diesel combustion in a single cylinder compression ignition engine. *Int. J. Hydrogen Energy* **2021**, *46*, 35495–35510. [CrossRef]